International Conference on Space Situational Awareness

Tres Cantos - Madrid, Spain

COMPARING THE EFFECTIVENESS OF POSITIONAL ACCURACY IMPROVEMENTS FOR SSA

Oltrogge, D.L.[(1)], Alfano, S.[(2)], and Gist, R.G.[(3)]

[(1)] COMSPOC Corporation's Center for Space Standards and Innovation, 224 Valley Creek Blvd., Suite 210, Exton, PA 19341 USA, dan@comspoc.com

[(2)] COMSPOC Corporation's Center for Space Standards and Innovation, 224 Valley Creek Blvd., Suite 210, Exton, PA 19341 USA, salfano@comspoc.com

[(3)] COMSPOC Corporation's Center for Space Standards and Innovation, 224 Valley Creek Blvd., Suite 210, Exton, PA 19341 USA, rgist@comspoc.com

Keywords: Conjunction assessment; orbital accuracy; flight safety.

ABSTRACT

How accurate do SSA products need to be for flight safety? Is there "too much accuracy," that is, is the added cost of further improving SSA accuracy warranted? In this paper, we explore these questions in several ways: (1) we review the encounter rate squared relationship for miss distance screening; (2) we examine the reduction of collision probability-based encounter rates stemming from positional accuracy improvements; and (3) we examine the applicability and effectiveness (in terms of Type I and Type II error statistics) of both miss distance and probability-based trending as a viable tool for collision avoidance maneuver go/no-go decision making.

1. Introduction

Our previous research has underscored the squared relationship that exists between close approach (or "encounter") rates and predictive positional accuracy for a pair of conjuncting objects. If conjunction assessment were to be based purely upon miss distance screening and that miss distance threshold was intentionally selected to encompass the combined error ellipse major sigma, then the number of concerning conjunctions would roughly vary as the square of the error. This puts a premium upon obtaining accurate SSA information (both at orbit determination epoch as well as predictive errors), because a doubling of errors would admit four times as many conjunctions to evaluate and for which avoidance maneuvers may be conducted.

But many operators, especially in Low Earth Orbit (LEO), choose to use collision probability-based conjunction assessment screening to identify conjunctions of potential concern. Accordingly, we have shown how one can plug an SSA analyst's desired collision probability risk threshold into the basic collision probability formula to select a conjunction screening miss distance pre-filter that ensures that all potential collisions that might exceed a selected risk threshold are retained. A collision probability algorithm of the analyst's choosing can then be applied to the remaining set of conjunctions to determine if the Pc threshold is exceeded.

But for this collision probability assessment procedure, what is the benefit of having higher accuracies of SSA positional knowledge? Researchers have asked similar questions in the past [1], focusing on catastrophic collision events using predefined positional covariances for different orbit regimes. Our analysis differs in that we use individual covariances for each and every object in the public catalog to assess both physical and probabilistic annual encounter rates as determined by our volumetric encounter rate tool. Our goals herein are to analyse the current spectrum of both miss distance and collision probability-based avoidance strategies against the current space population, especially focused upon collision probability thresholds employed by today's spacecraft operators.

If we equate operator workload to the number of conjunctions that require Flight Dynamics Staff (FDS) analysis and intervention, does that workload reflect the collision probability concepts of the "robust region," "max probability region," and "dilution region?" Is there an encounter rate equivalency to the collision probability topology that has previously been identified?

In this paper, we will statistically characterize collisions by altitude, latitude, miss distance distribution, annual collision rates, combined error, and combined hard body radius. Next, we will review the miss distance screening, and the corresponding encounter rate squared relationship shown in our previous research and investigate how being able to justify using smaller miss distance thresholds eliminates collision avoidance analysis work. And finally, we will explore the dependencies of collision probability-based encounter rates and collision risk mitigation effectivity as positional accuracy and collision probability screening thresholds change.

2. Establishing the foundational elements

To evaluate the effectiveness of SSA information, we first need to characterize the following in this section:

- Covariances for all public space objects
- Typical covariance accuracy of SSA positional knowledge
- Volumetric characterization of encounter rates
- Typical hard body size and inclination as a function of altitude

2.1. Typical accuracy of SSA positional knowledge

Knowledge of the typical (or median 50th percentile) uncertainty covariance of satellites and debris objects enables the computation of typical collision probability using classic collision probability assessment approaches as well as estimating the chances of occupying a common volume. Obtaining and integrating this covariance information directly from individual operators is logistically difficult, and for debris objects the problem is even more difficult.

To work around these challenges, our study makes use of a covariance for each resident space object (RSO) derived from statistical accumulation of differencing between actual position/velocity predictions and observations, which is termed ***synthetic covariance***. COMSPOC's method for obtaining synthetic covariance is well documented in [2]. Such a synthetic covariance is especially useful since it is based on freely available data for all publicly available RSOs without delay, it uses well-understood propagation models, it shows an operationally realistic evaluation of observable uncertainty, it is adaptive to operational and environmental changes over time, and the reference frame and coordinate system will be uniform for all objects.

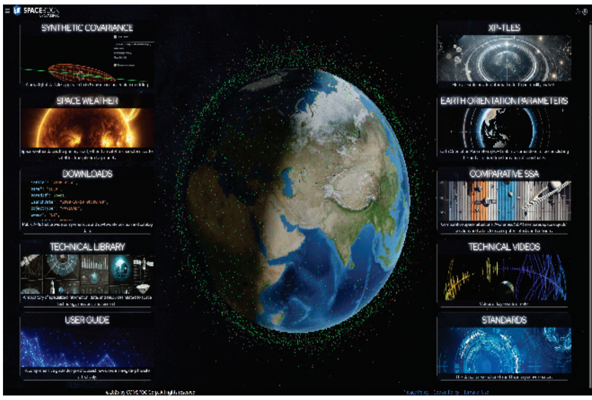

Figure 1: Spacebook.com portal contains a wealth of space information.

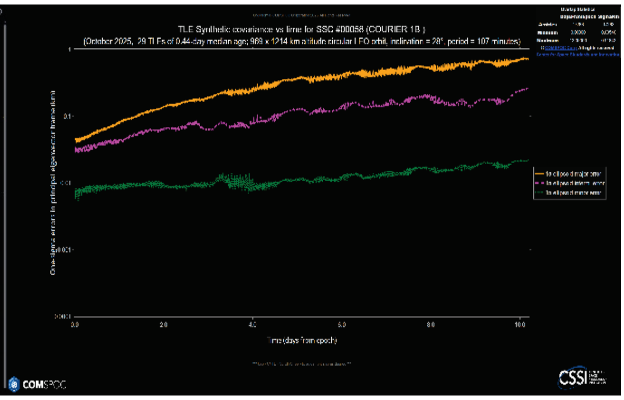

Figure 2: Sample major, intermediate, and minor one sigma dimensions for TLE RSO.

An obvious source of observations to feed this synthetic covariance generation process is the comprehensive data from the US government in the form of two-line element sets (TLEs) and the more accurate data from their Special Perturbations model (SP). Daily synthetic covariance for each unclassified RSOs is currently being generated from both TLE and SP data sources by COMSPOC and is available via their Spacebook website[12], shown in **Figure *1*** with a sample plot of minor, intermediate, and major sigmas versus time for all public TLE and SP products shown in **Figure 2**.

The generation of synthetic covariance is described fully in this reference[2]. In brief, the process is as follows. For each RSO, the most recently available orbit element set is propagated forward over a preset time span. Prior orbit elements sets are propagated forward to overlap this time span. Position and velocity differences are computed between these earlier propagations and the current one in an orbit relative coordinate frame with in-track, cross-track, and anti-nadir components. Statistics are accumulated within bins based on time from epoch and argument of latitude. A sliding weighting scheme is used to blend statistics over time, emphasizing more robust overlapping regions (only a week or two in the past), and gradually de-weighting much older overlap statistics and de-weighting more recent, but sparser, overlap statistics. Any gaps in statistical bins are filled via bilinear interpolation from neighbouring data.

2.2. Typical accuracy of SSA positional knowledge

COMSPOC's synthetic covariance [2, 3] process yields dynamic distribution files that log the statistics of sequential overlaps binned by time and argument of latitude. Those files proved to be extremely useful for this analysis, as they allowed the median covariance to be determined for each individual object, as well as collections of objects binned by activity status and altitude.

2.3. Size/dimensions of Resident Space Objects

A second necessary but often overlooked data input required to assess collision probability is the size of all RSOs in space. There are multiple ways to portray RSO size: “equivalent” radius, physical dimensions, “radius of a minimally encapsulating sphere”, “Optimally Enclosing Box (OEB). Note that there may be multiple definitions corresponding to the commonly used term, “Hard Body Radius” or HBR: It could refer to the equivalent radius which presents the same Cross-Sectional Area (CSA) as the median CSA of a tumbling object of arbitrary orientation as computed in [4], or HBR could represent a “conservative,” overly-large CSA corresponding to a minimally-encapsulating sphere.

One valuable, globally available source of such information is the **DISCOS database** [5], which houses such essential information as spacecraft shape, size, and mass. But as it turns out, DISCOS only contains non-blank size information for 19344 of the 29668 TLEs in the current public catalog. Naturally, that raises the question of what default value(s) to use for the 35% of RSOs for which a value is not provided. We had two schools of thought:

(1) Since ESA likely can get rough sizing information for the larger RSOs, in particular, families of objects such as upper stage spent rocket bodies, large constellation spacecraft, and types of earth observing spacecraft, perhaps it is likely that the smaller (but still trackable) debris objects cannot be well characterized, and since the Space Surveillance Network can track down to roughly 5 to 10 cm, we adopted a value of 7.5 cm for an HBR.
(2) Since we noticed that some rocket bodies (which are quite large) did not have values, it was felt that perhaps 7.5 cm was too small to be used as a default for the population, so we also used 1m HBR.

In the end, recognizing that both values were not perfect, we decided to run both of those cases and share results for both. In this manner, we can learn how sensitive our results are to these default values.

Shortly before presentation of this paper, the Office of Space Commerce announced [6] that it had published a "conjunction assessment dataset," developed for the **Traffic Coordination System for Space** (TraCSS), to help space situational awareness service providers test their conjunction assessment algorithms. This database includes an RSO size file based, at least in part, upon the Space Flight Safety Handbook (which we will label hereafter as SFSH). This size file includes HBRs for 24108 RSOs in the public catalog, still leaving 19% of current RSOs without size information (again, requiring use of default value(s) to be used).

catalog_num	HBR	ScreeningVolume	U (km)	V (km)	W (km)
5	0.0825	SFS Handbook Table 3 LEO2	0.4	25	25
11	0.254	SFS Handbook Table 3 LEO2	0.4	25	25
12	1.0308	SFS Handbook Table 3 LEO2	0.4	25	25
16	1.0308	SFS Handbook Table 3 LEO2	0.4	25	25
20	0.254	SFS Handbook Table 3 LEO2	0.4	25	25

Unfortunately, there was no accompanying description of what “flavour” of HBR this data adopted: was it a radius representing an equivalent cross-sectional area, or was it an encompassing sphere, or was it representing the median (“typical”) cross section? To help ascertain how this size file defines HBR, we computed the distribution and CDF of the SFSH sizes ratioed to the DISCOS median values as shown in **Figure 3**. As shown, the typical ratio (at the 50th percentile of the CDF, righthand axis) was two, indicating a substantial mismatch between DISCOS medians and the SFSH HBR values.

This led us to try instead a DISCOS-based encompassing sphere, which we found matched quite well with SFSH with a ratio of 1.1 (see **Figure 4**). We conclude, without further confirmation or proof, that the SFSH database appears to represent HBRs of encompassing spheres about each RSO. Assuming that to be the case, it means that any flight safety conducted (even in “simulation mode” as OSC intended the data to be used) would incorporate equivalent cross sectional areas that are a factor of two larger than DISCOS-based median values, which will greatly influence the rates of encounter and effectivity of the collision avoidance process.

One final note: while **Figure 4** typically matches well with the DISCOS database, there are plenty of cases where HBRs are off by factors of up to 50X or so. This further underscores the urgent need to build as accurate an understanding of RSO equivalent cross-sectional areas as possible, ideally consensus-driven across the global space community.

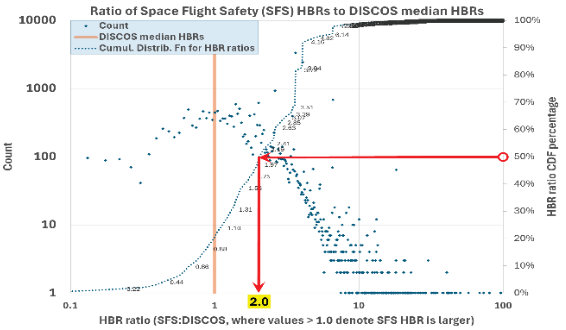

Figure 3: Ratios of SFSH and DISCOS median HBR values indicate a typical factor of two difference (poor match).

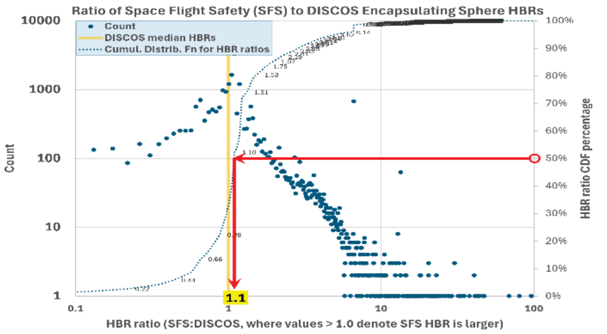

Figure 4: Ratios of SFSH and DISCOS Encompassing Sphere HBR values indicate a fair match, indicative of SFSH representing Encompassing Spheres.

2.4. Volumetric characterization of encounter rates

COMSPOC’s volumetric encounter method [7] was used to estimate the rate of both close encounters as well as collisions. The volumetric approach has been well validated in the operational context against real-world conjunctions [8, 9, 10]. The distance-based annual encounter rate is determined from the volumetric tool [7] by assuming a spherical encounter volume sized to the Cartesian screening threshold.

The sphere’s movement along a satellite's circular or elliptical orbit sweeps out a path-centred, circular, cross-section ring torus. Should the other satellite’s path pierce this torus, then an encounter occurs. One then determines the time spent in the torus relative to the orbital period. Because along-track position is assumed to be uniformly distributed in mean anomaly for both orbits, this ratio is then used to determine the annual distance-based encounter rate.

Applying the volumetric encounter method to all pairs of RSOs in the entire public catalog as of 20 February 2026 yields **Table 1**. As shown, the active-on-active collision risk is relatively low if all spacecraft operators avoid performing “fratricide,” defined as one spacecraft of a constellation hitting another in-constellation satellite.

Table 1: 2026 collision rates by regime and activity ((DISCOS, 7.5cm gap-fill)

	LEO	MEO	GEO	XGEO	All
Debris-on-Debris	0.20	2.2E-04	1.0E-04	1.1E-04	0.20
Active-on-Debris	1.26	7.9E-05	8.0E-04	6.6E-06	1.26
Active-on-Active with fratricide	47.30	4.0E-04	7.1E-03	1.8E-06	47.30
Active-on-Active, no fratricide	2.24	4.0E-04	7.1E-03	1.8E-06	2.24
All activity combinations with fratricide	48.70	6.9E-04	8.0E-03	1.2E-04	48.70
All activity combinations, no fratricide	3.70	6.9E-04	8.0E-03	1.2E-04	3.71

Some are quick to point out that it is unnecessary to include the fratricide case; however, this would be our actual collision risk in the event of an en masse extinction of large constellation spacecraft due to a Carrington event, a nuclear detonation (NuDet) in space, or other threats recently reported in the press regarding potential bad state actor actions to use lethal force against spacecraft constellations.

Summarizing Table 1 (default HBR 7.5 cm), we anticipate in the 2026 era:

- **Collisions may occur every five years** between two publicly tracked debris objects.
- **If fratricide is not effectively prevented, 47 collisions may occur annually.**
- **Excluding fratricide, two hardbody collisions may occur annually** involving two publicly tracked and acknowledged active spacecraft *if inter-operator collision avoidance procedures and SSA data render collision avoidance ineffective*.

More than one collision would occur annually between an active spacecraft and debris if operators and SSA systems do not effectively (a) identify the collision risk; and (b) mitigate that risk.

Table 1 was achieved by using the median equivalent HBR values derived from the DISCOS database. Unfortunately, dimensions for a substantial portion of the public catalog objects were not available in DISCOS, forcing us to adopt a “gap-filling” default HBR of 7.5 cm in those cases

Next, we found that adopting a 1m default HBR, as shown in **Table 2**, had a dramatic impact on the rates of collision for debris-on-debris and active-on-debris.

Table 2: 2026 collision rates by regime and activity (DISCOS, 1m gap-fill HBR)

	LEO	MEO	GEO	XGEO	All
Debris-on-Debris	0.77	3.0E-04	1.1E-04	1.1E-04	0.77
Active-on-Debris	1.63	8.4E-05	8.1E-04	6.7E-06	1.63
Active-on-Active with fratricide	47.30	4.0E-04	7.1E-03	1.8E-06	47.30
Active-on-Active, no fratricide	2.24	4.0E-04	7.1E-03	1.8E-06	2.25
All activity combinations with fratricide	49.70	7.9E-04	8.0E-03	1.2E-04	49.70
All activity combinations, no fratricide	4.64	7.9E-04	8.0E-03	1.2E-04	4.65

And finally, the SFSH HBRs were applied, resulting in the expected collision rates shown in**Table 3**. Notice how the aggregate collision rates increased by a factor of five or six, which is reasonably close to two squared, especially considering that some of the ratios were as high as 50X higher.

Table 3: 2026 collision rates by regime and activity (SFSH, 1m gap-fill HBR)

	LEO	MEO	GEO	XGEO	All
Debris-on-Debris	0.82	1.5E-03	5.7E-04	7.1E-04	0.82
Active-on-Debris	6.76	5.7E-04	5.1E-03	4.1E-05	6.77
Active-on-Active with fratricide	245.00	2.5E-03	4.9E-02	9.6E-06	245.00
Active-on-Active, no fratricide	13.20	2.5E-03	4.9E-02	9.6E-06	13.2
All activity combinations with fratricide	253.00	4.6E-03	5.5E-02	7.6E-04	253.00
All activity combinations, no fratricide	20.70	4.6E-03	5.5E-02	7.6E-04	20.80

2.5. Typical RSO size

Typical space object size was evaluated by enveloping the satellite in a rectangular box (as opposed to an encapsulating sphere) and then using the median projected box's area to define an equivalent hard body radius [11]. These values are based upon ESA's DISCOS database [5] We observed that DISCOS occasionally does not provide width, height, depth, diameter, span, or cross-sectional area information for some objects. For these we were forced to choose default values mentioned previously. This data is provided freely on the SPACEBOOK website [12].

3. Statistical characterization of collision risk by altitude and activity status

Before examining SSA effectiveness, let us characterize the conditions where collision threat exists. In this section, we will examine the altitude, latitude, miss distance, combined error, and combined hard body radius for all identified collision risk RSO pairs in the public catalog, for the following combinations and categories:

- Active-on-Active
- Active-on-Debris
- Debris-on-Debris
- Orbital regime (LEO, MEO, GEO, XGEO)

Assumptions: These statistics were generated by applying the Volumetric Encounter Rate tool to all pairs of RSOs in the publicly tracked TLE catalog from 20 February 2026. Rates from fratricide (particularly within large constellations) were excluded for the Iridium, Starlink, OneWeb, and Amazon LEO (formerly Kuiper) constellations.

Distributions were binned using 8000 altitude bins, 1000 bins for miss distance and a proxy for combined positional accuracy (computed as the summation of 1σ errors along the error ellipsoid major principal axes for both conjuncting RSOs), and 200 bins for latitude and combined hardbody radius. Within each bin, the summation of collision rates was performed (excluding fratricide).

In **Figure 5** through **Figure 14**, characterizations in both LEO and GEO are provided altitude, latitude, miss distance distribution, annual collision rates, combined error, and combined hard body radius. Noteworthy things to observe include the strong altitude dependence on active-on-actives, active-on-debris, and debris-on-debris in LEO. GEO is dominated by active-on-active collision risk as a percentage of total GEO risk. Debris-on-debris dominates the collision risk in LEO above 800 km and below OneWeb's 1200 km, while collisions involving at least one active space object dominate elsewhere in LEO. Debris-on-debris collision risk (based upon the tracked public catalog) is virtually non-existent in GEO. Active satellites have significantly more error than debris, presumably due to the extensive accuracy degradation that maneuvers cause. Active-on-active GEO collision risk typically has a combined hardbody radius of 10 meters.

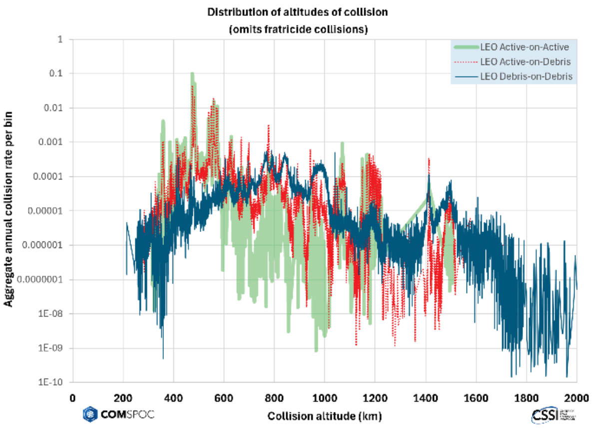

Figure 5: *Distribution of LEO collision altitudes weighted by collision rate.*

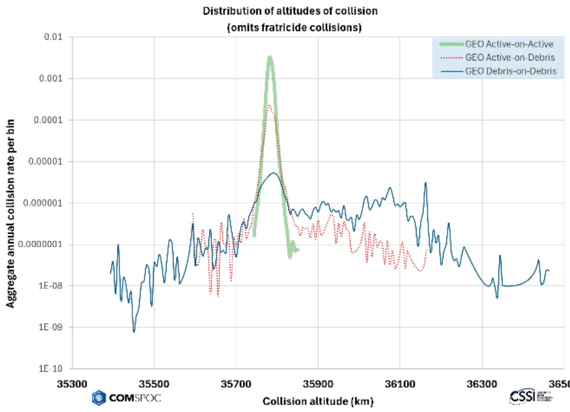

Figure 6: Distribution of GEO collision altitudes weighted by collision rate.

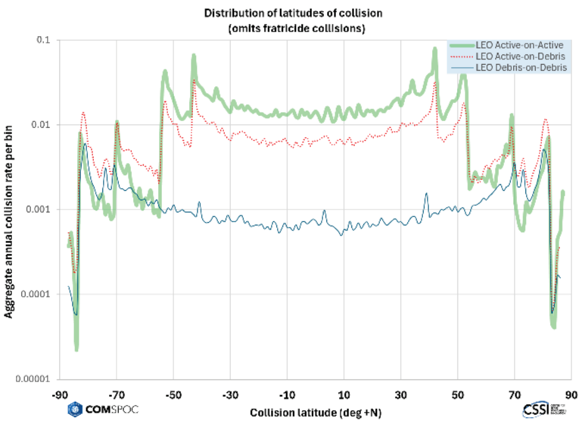

Figure 7: Distribution of LEO collision latitudes weighted by collision rate.

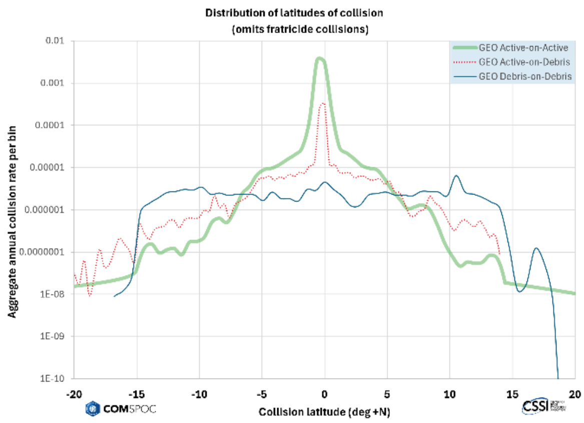

Figure 8: Distribution of GEO collision latitudes weighted by collision rate.

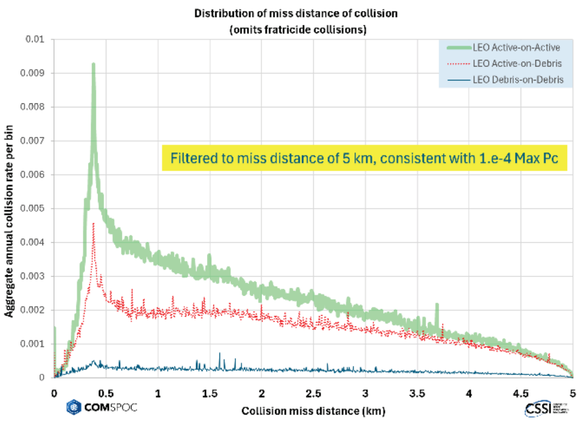

Figure 9: Distribution of LEO collision distance weighted by collision rate.

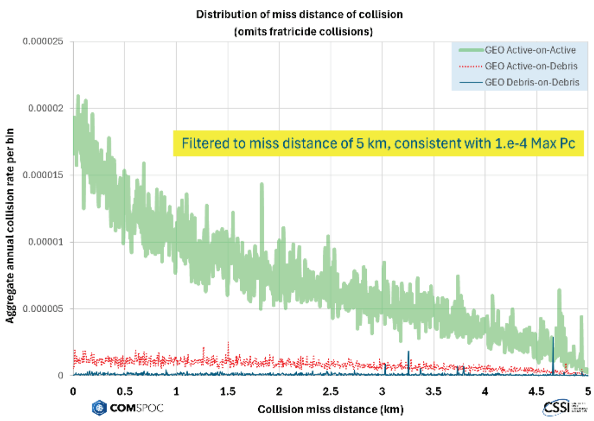

Figure 10: Distribution of GEO collision distance weighted by collision rate.

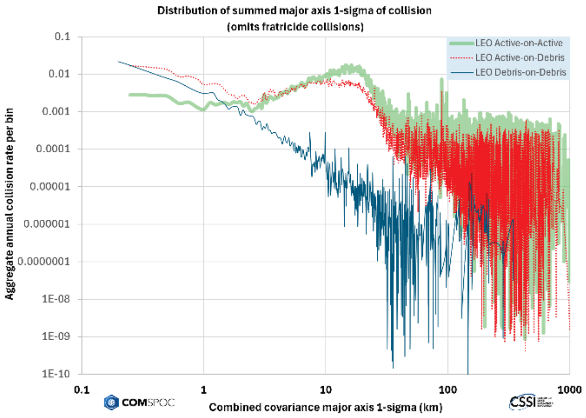

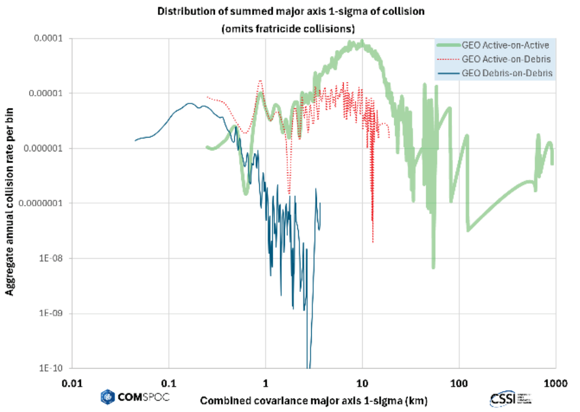

Figure 11: Distribution of LEO collision 1σ sums weighted by collision rate.

Figure 12: Distribution of GEO collision 1σ sums weighted by collision rate.

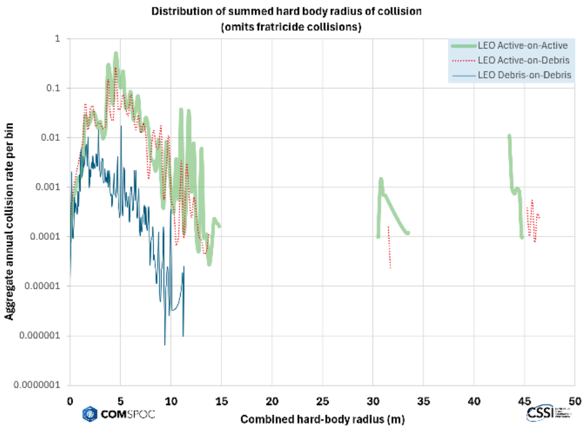

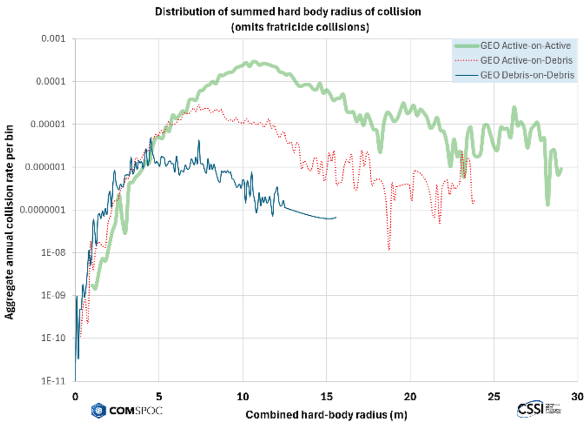

Figure 13: Distribution of LEO collision combined HBRs weighted by collision rate.

Figure 14: Distribution of GEO collision combined HBRs weighted by collision rate.

4. Miss distance screening

Some operators use miss distance as the sole approach to avoiding collisions. A survey[11] that we conducted jointly with the Space Data Association and its spacecraft operator members indicated that while many use collision probability in LEO, miss distance, or at least componentized miss distance (radial component thresholds, for example) can dominate in other regimes.

We have previously shown that the rates at which an object comes close to another varies as the square of the screening distance being used [13]. For example, note the log-linear strong relationship shown in **Figure 15** for the 71-satellite Iridium constellation. It turns out that this relationship is an important one for miss distance screening, because it means that if the operator can justify using a much smaller miss distance screening threshold by having substantially more timely and more accurate SSA data, the fewer the number of predicted conjunctions (and subsequent collision risk) the operator must deal with.

It is unclear how typical miss distance screening analysts and operators select their miss distance thresholds. We have also shown that by padding miss distance screening thresholds, the analyst can eliminate Type II (false negative) errors [14]. One suggested approach is to base the miss distance screening threshold on any insights one can obtain on the accuracy of the SSA data feeding the miss distance screening. For example, if a typical 1σ error for RSOs in the orbit regime in question is approximately 1 km and we also know that a 3-dimensional 1σ error covariance only encompasses 19.9% of the error ensemble, then it might be logical to conservatively add the two 1σ values together and multiply by three to obtain a miss distance that conservatively encompasses a combined 3σ error volume (which in turn contains 97.1% of the error ensemble).

But a somewhat more rigorous approach is provided in [20], which allows the user to "reverse engineer" a maximum probability-based miss distance that helps to ensure that the selected miss distance is well-suited to catch all conjunctions of potential concern.

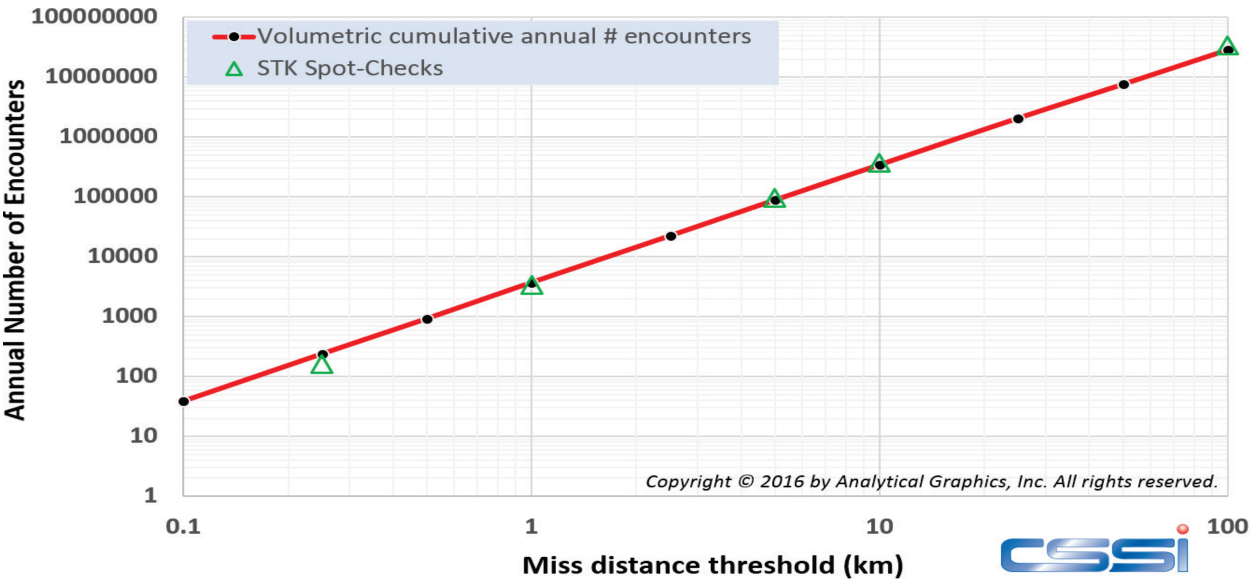

Figure 15: ***Sample comparison of volumetric encounter method and high-fidelity simulations for the Iridium constellation.***

5. Annual encounters for probability-based screening

Other operators don't use miss distance screening, instead choosing to use probability-based assessment screening, especially in Low Earth Orbit (LEO), to identify conjunctions of potential concern. To compute this probability, we use an SSA analyst's desired collision probability (risk) threshold ($P_{threshold}$) to define an alert region in Mahalanobis [15] space. This is done using a basic collision probability formula to create a Mahalanobis screening distance. This ensures that all potential collisions that might exceed a selected risk threshold are retained if the actual Mahalanobis distance between two objects is at or below that distance.

For this study, the orbital data and associated covariances plus hard-body radii freely provided by [12] were used. The website's covariances are determined synthetically[2] and the hard-body radii are derived from the DISCOS database's satellite dimensions. With these data, much of the analysis that follows is accomplished in the Mahalanobis space[15].

The Mahalanobis space is an isotropic space where each axis is scaled to have unit variance. In this space, also known as the sigma space, the two-dimensional miss distance becomes the unitless parameter dm represented as in **Eqn. 1**:

$$dm = \sqrt{\left(\frac{xm}{\sigma x}\right)^2 + \left(\frac{ym}{\sigma y}\right)^2} \quad (1)$$

where x lies along the covariance ellipse minor axis, y lies along the major axis, xm and ym are the respective components of the projected miss distance in the encounter plane in Cartesian space, and σx and σy are the corresponding standard deviations. Accordingly, the combined hard-body radius *r* becomes *rm as in **Eqn. 2**:*

$$rm = \frac{r}{\sqrt{\sigma x \sigma y}} . \quad (2)$$

Mahalanobis distance screening is achieved by measuring how many standard deviations away the combined object's centre is from the combined, covariance ellipse centre.

As described in our previous work [16], Chan [17] developed an analytical approximation for probability by rescaling the problem to circularize the covariance error ellipse thereby making the projected, combined, hard-body object footprint an ellipse. He then replaced this object ellipse with a circle of equivalent area as shown in **Figure 16** where the size of *rm* relative to *dm* is greatly exaggerated for illustration purposes.

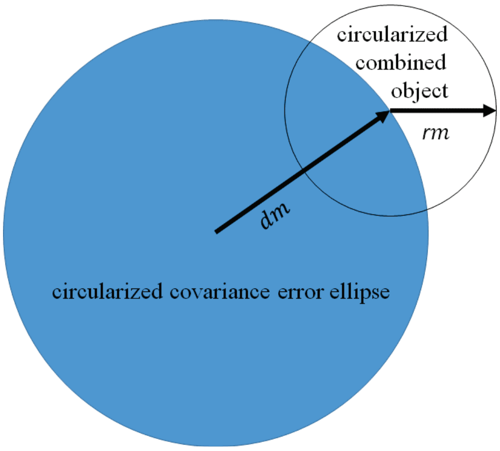

***Figure 16**: Chan's approximation*

To complete his approximation, Chan transformed the Gaussian PDF to a Rician PDF. For this analysis, such a transformation is unnecessary. In the Mahalanobis space depicted in **Figure 16**, collision probability *Pc* is found using Chan's simplifying **Eqn. 3**:

$$\mathrm{P}_c(dm, rm) = e^{-\frac{1}{2}[dm^2]}(1 - e^{-\frac{1}{2}[rm^2]}) \quad (3)$$

To determine the Mahalanobis distance screening threshold (dm_{alert}) based on the probability screening threshold ($P_{threshold}$) we solve **Eqn. 3** by substituting dm_{alert} for dm as in **Eqn. 4**:

$$dm_{alert}(\mathrm{P}_{threshold}, rm) = \sqrt{-2(\ln\left[\frac{\mathrm{P}_{threshold}}{1- e^{-\frac{1}{2}[rm^2]}}\right])} \quad (4)$$

Given an alert screening distance threshold dm_{alert} measured in sigma units in the encounter plane sigma space, **Eqn. 3** is used to determine the probability of the object centre being within that distance where $dm <= dm_{alert}$ results in an alert. The greater the Mahalanobis screening distance, the less likely it is that an analyst wouldn't be notified of an actual collision event. If the screening distance is zero, then all alerts will be discarded except for the extremely unlikely case of a direct, center-to-center hit, leading to many missed alerts.

This Mahalanobis approach is not limited to alert screening, lending itself to examining other actionable probability thresholds and their corresponding Mahalanobis distances and errors. Such actions beyond alert warning could take the form of planning a maneuver, executing a maneuver, modifying a station-keeping schedule, or simply monitoring conjunction progression prior to TCA by taking observations more frequently and/or from different sources to refine the assessment.

The next step is to determine the distance-based annual encounter rate from our volumetric tool[7] as previously described. Using both a 5km and 60km screening radius, we determine if a conjunction is possible. The 5km screening radius is used to determine the local miss distance-based collision rate as well as to characterize the possible collisions on the basis of altitude, latitude, etc. The 60km radius was determined for an aspect ratio of 10 and hardbody radius of 30m that would produce a maximum probability just under 10e-6. If yes, we determine if the probability threshold has been exceeded. If both are true, we take the distance-based conjunction rate and find the corresponding probability-based rate. As shown in Reference [7], the collision rate is directly proportional to the square of encounter radius. For example, a reduction by one order of magnitude in the encounter radius yields a reduction in encounter rate by two orders of magnitude. With this knowledge we can scale the distance-based rate by using the ratio of dm_{alert} to the 5km and 60 km Mahalanobis length along the miss-distance vector to produce a probability-based rate.

This analysis is repeated with different sigma scale factors ranging from 0.01 to 10.0 to show the effect of covariance size on the rate of specified probability threshold exceedance as shown in **Figure 17**. The green line with triangle markers represents a one in ten thousand Pc threshold. For this assessment, we used the volumetric encounter tool to identify all space object pairings in the public catalog involving at least one debris piece (i.e., active-versus-debris and debris-versus-debris) which could have the potential to conjunct within 60 km. We did not include active-versus-active because here we assumed that fratricide would be successfully prevented by each operator.

Figure 17 shows, for four collision probability thresholds ranging from one in one thousand to one in one million, that probability-based (Pc threshold exceedance) encounter rate increases as the covariance improves (shrinks) from the righthand side towards the left, reaches a peak, and then drops. This behaviour can be explained using the concept of maximum probability and dilution [18] where a pseudo-"maximum probability" ridge line is observed in aggregate across the entire

RSO catalog as shown in **Figure 18**, with the green colour crudely denoting the "robust region" and the pink colour denoting the "dilution region."

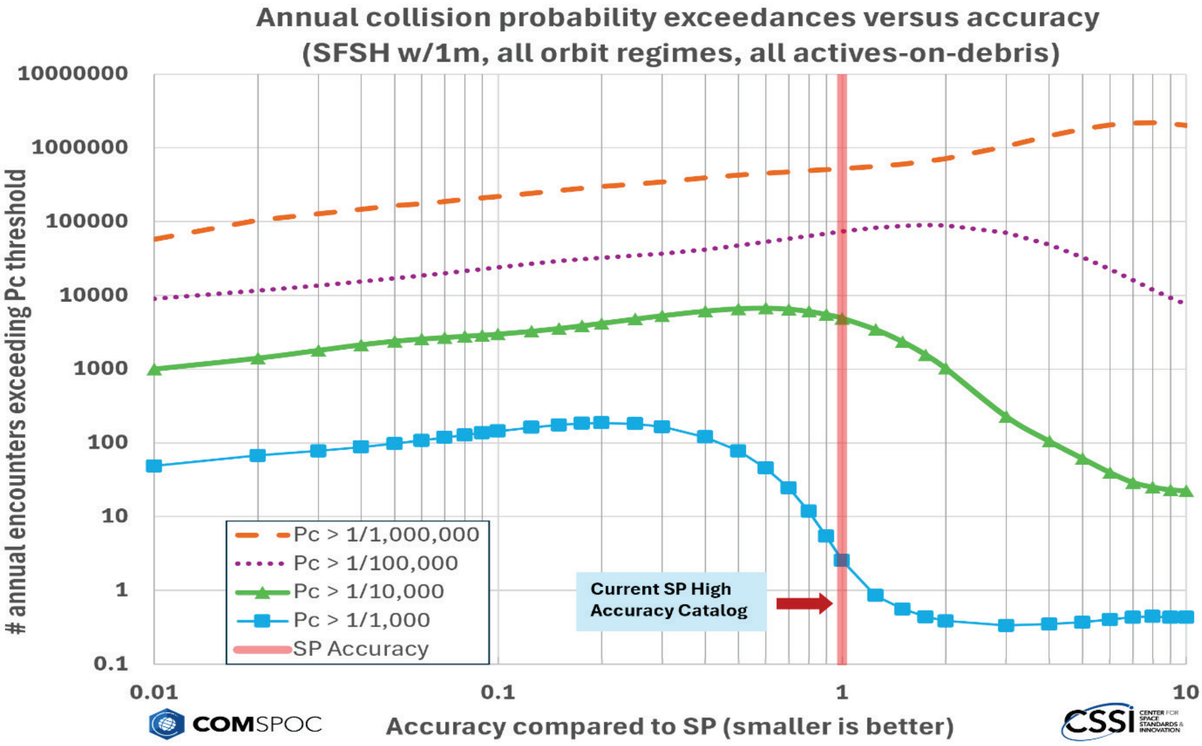

Figure 17: Annual rate of collision probability exceedance vs. scale factor and four Pc thresholds

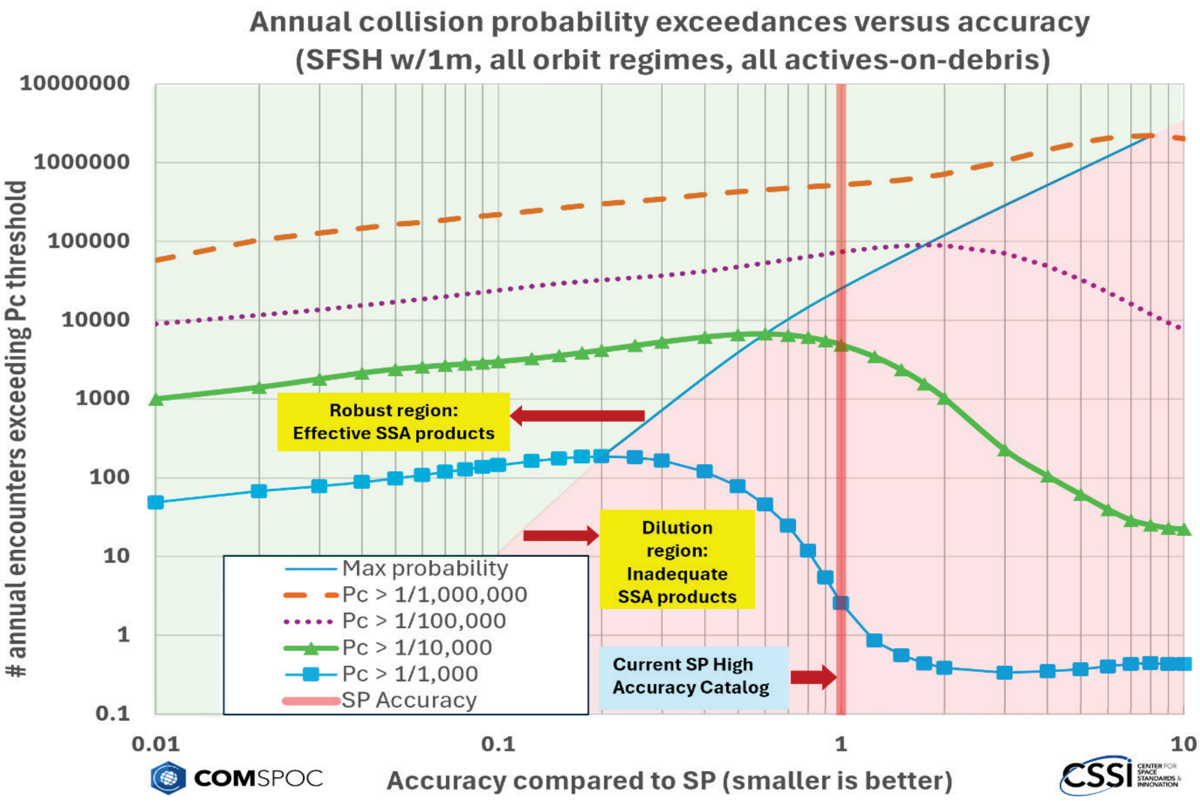

Figure 18: Annual Pc exceedance rate vs scale factor, depicting robust and dilution regions

For fixed object sizes and Cartesian miss distance, the combined-covariance minor-axis standard deviation (σ_x) that produces the maximum probability (*Pmax*) defines the dilution region boundary as shown in **Figure 19**. To the left of the vertical line, lesser positional uncertainty (smaller σ_x) decreases collision probability.

To the right of the vertical line, larger positional uncertainty (greater σ_x) also decreases collision probability. Both small and large uncertainties can produce the same mathematically correct probability (10^{-6} is given as an example in **Figure 19**). A very large uncertainty indicates little confidence in the predicted miss distance and will result in a low probability, absurdly suggesting that satellite safety increases as data quality decreases. It is only one's awareness of real collision threats that decreases.

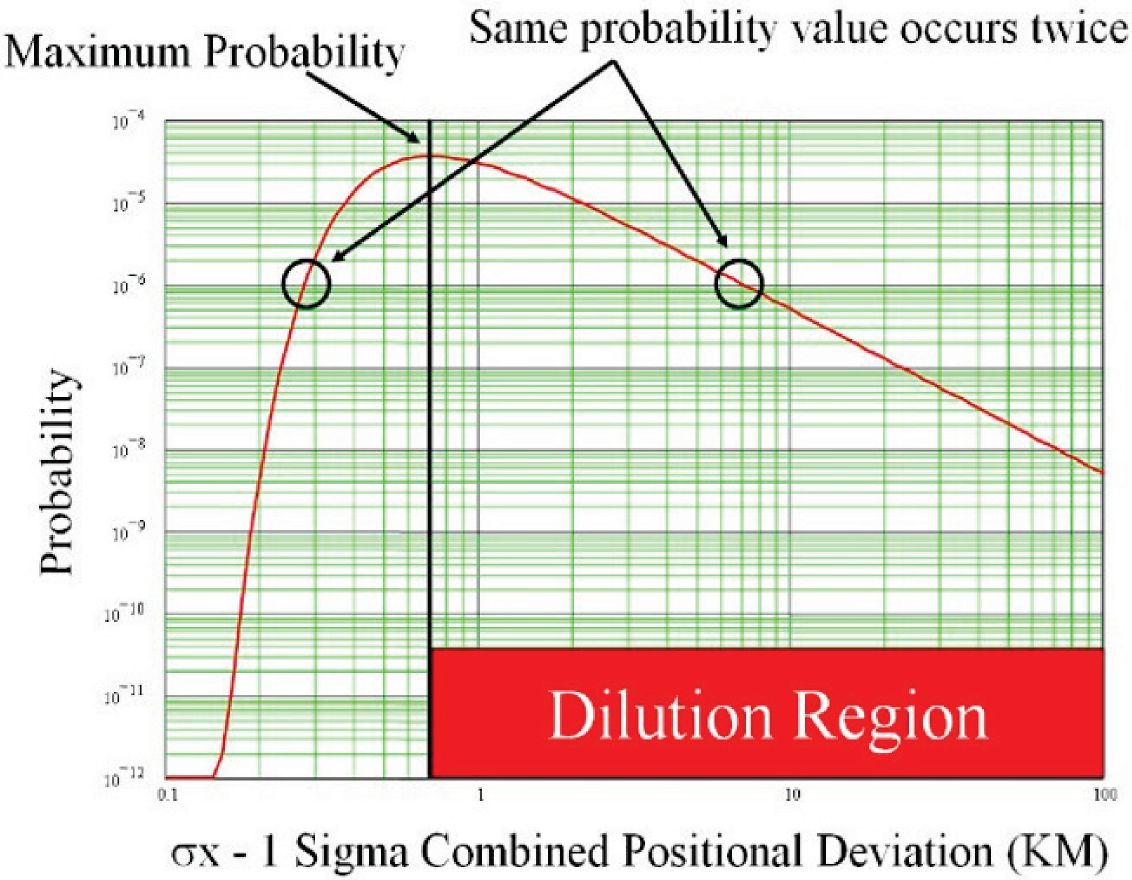

Figure 19: Dilution Region Defined for Notional Encounter

Probability-based screening is predicated on positional uncertainty being properly characterized. If so, and if the calculated (true) probability is above an action threshold, then action could (and should) be taken regardless of whether the calculation occurred in the dilution region.

But if the calculated (true) probability is below the action threshold, two cases present themselves: (1) one can infer there is no threat with great surety in the robust region because the low probability is coupled with great confidence in the predicted miss distance; and (2) in the dilution region, the user might erroneously conclude that a particular encounter does not pose a worrisome threat simply because SSA accuracy is poor and there is little confidence in predicted miss distance.

6. What can we deduce from this Pc exceedance characterization?

We know from previous pathfinders and demonstrations that a deep collaboration between government and commercial SSA systems coupled with spacecraft operator sharing and involvement that it is possible (though challenging) to achieve a tenfold improvement in positional accuracy over legacy SSA system products. **Figure 20** shows, for a sample GPS spacecraft, a three- to tenfold improvement in positional accuracy is achievable over SP and TLE legacy SSA products, while **Figure 21** shows a tenfold improvement over both SP and TLE products in GEO.

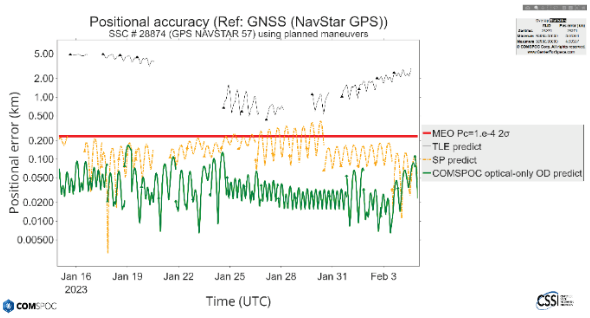

Figure 20: Comparison of legacy versus commercially fused SSA accuracy using GPS third-party reference ephemeris.

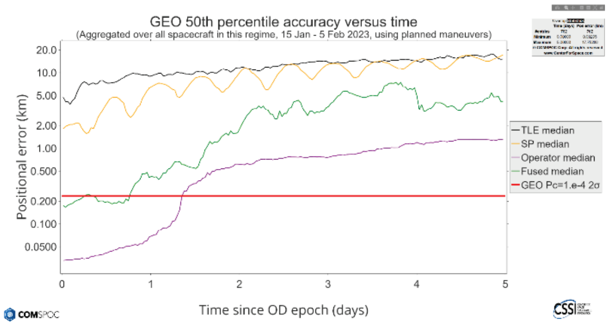

Figure 21: Statistically aggregated comparison of legacy versus commercially fused GEO SSA accuracy.

Accordingly, in **Figure 22**, we have labelled the number of annual probability exceedances one could anticipate for S=1 (legacy SP estimated accuracy), peak annual exceedances at the pseudo-max probability boundary, and the number of exceedances at S=0.1 (a tenfold improvement). The labelled annual rate numbers indicate that SSA centres and spacecraft operators could reduce the number of warnings 3X to 4X for performant collision probability screening thresholds (i.e., one in one hundred thousand or one in a million) if they could use SSA products that are a factor of ten more accurate than SP.

Faced with a low probability below the action threshold, one can use the dilution region boundary as a discriminator. If the positional uncertainty is not small enough to avoid the dilution region, then it would be prudent to attempt to reduce the positional uncertainty on both conjuncting space objects and reassess the true probability. If the uncertainty still yields a low probability below the action threshold in the dilution region, one should also consider the maximum probability (worst-case scenario for predicted miss distance) as well as the calculated one. This will help to ensure that a decision maker is not lulled into a false sense of security by a low probability calculation that may be specious.

Based on the above description, **Figure 22** indicates that the nominal (unscaled) SP covariances, taken in aggregate across the entire space population, are located well into the dilution region, particularly when using a one in ten thousand screening Pc threshold.

Corresponding annual collision probability exceedance charts for DISCOS and SFSH HBRs gap-filled with 1m default values are shown in **Figure 23** and **Figure 24**, respectively.

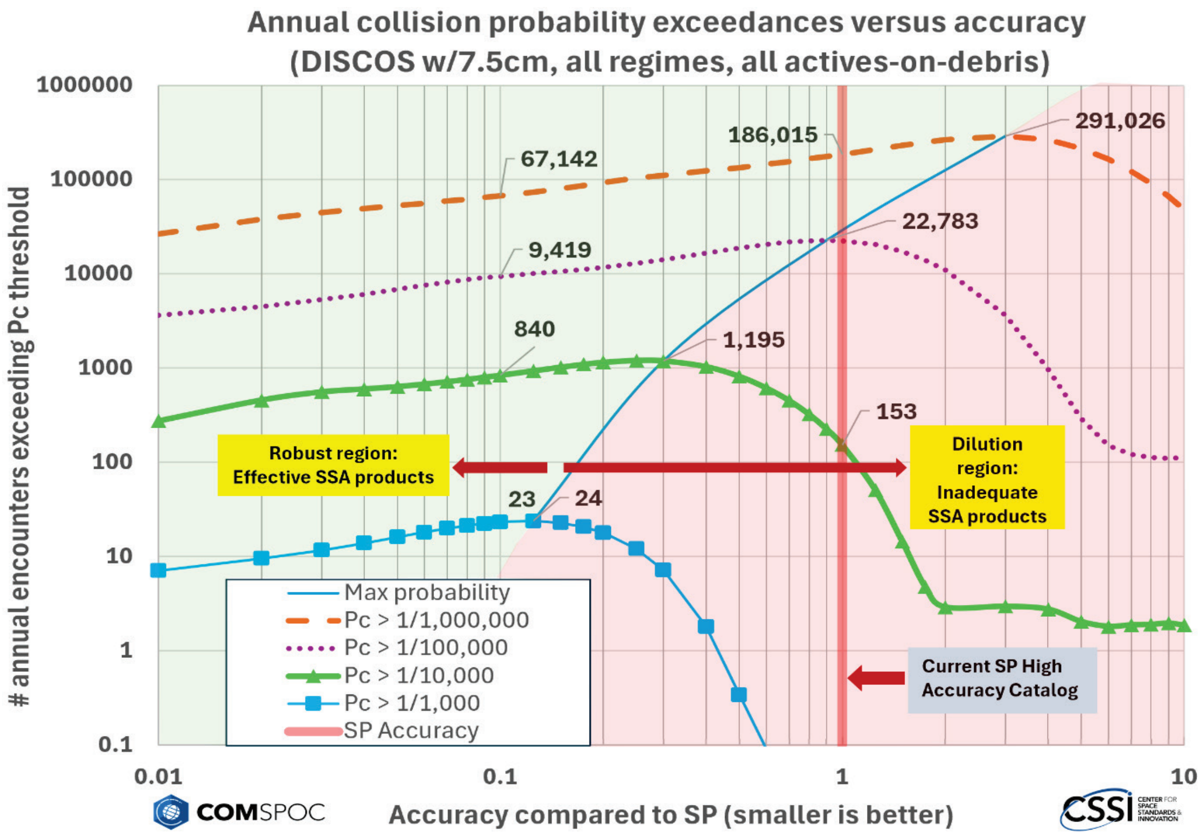

Figure 22: Annual Pc exceedance rate vs scale factor, depicting robust and dilution regions with numerical labels (DISCOS HBRs gap-filled with 7.5 cm)

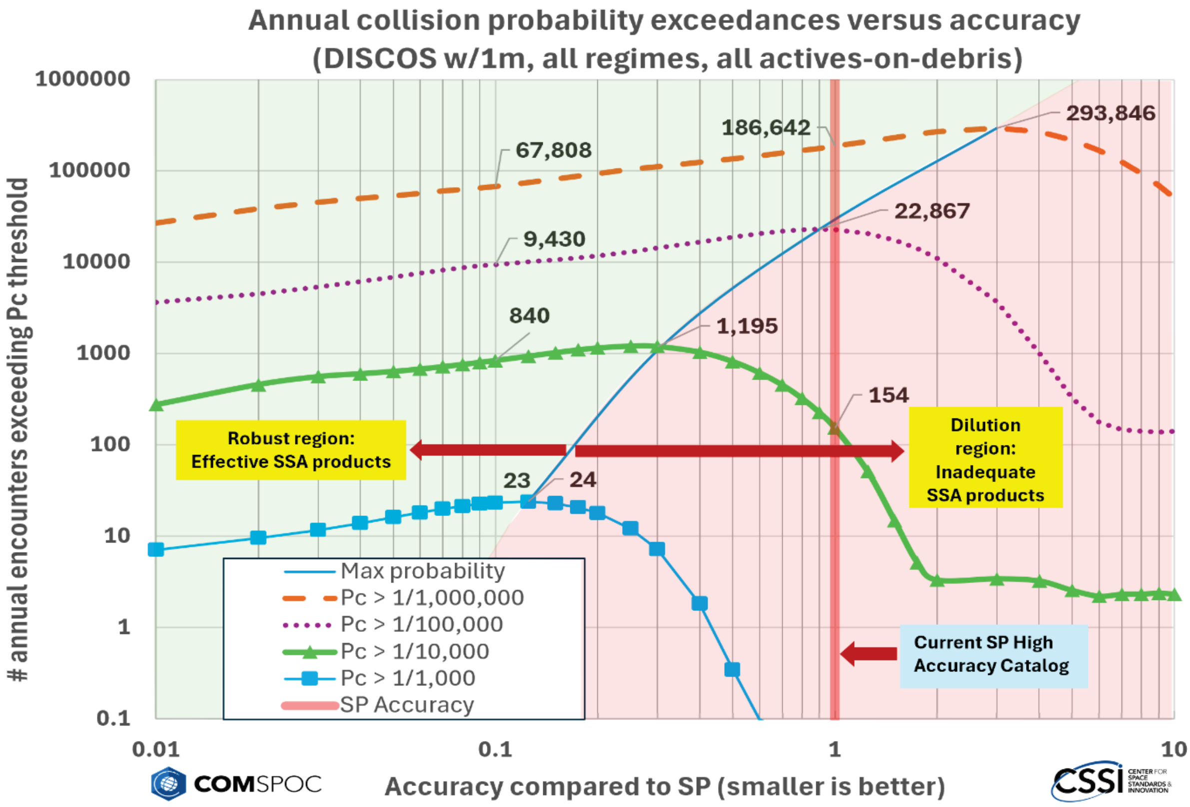

Figure 23: Annual Pc exceedance rate vs scale factor, depicting robust and dilution regions with numerical labels (DISCOS HBRs gap-filled with 1m)

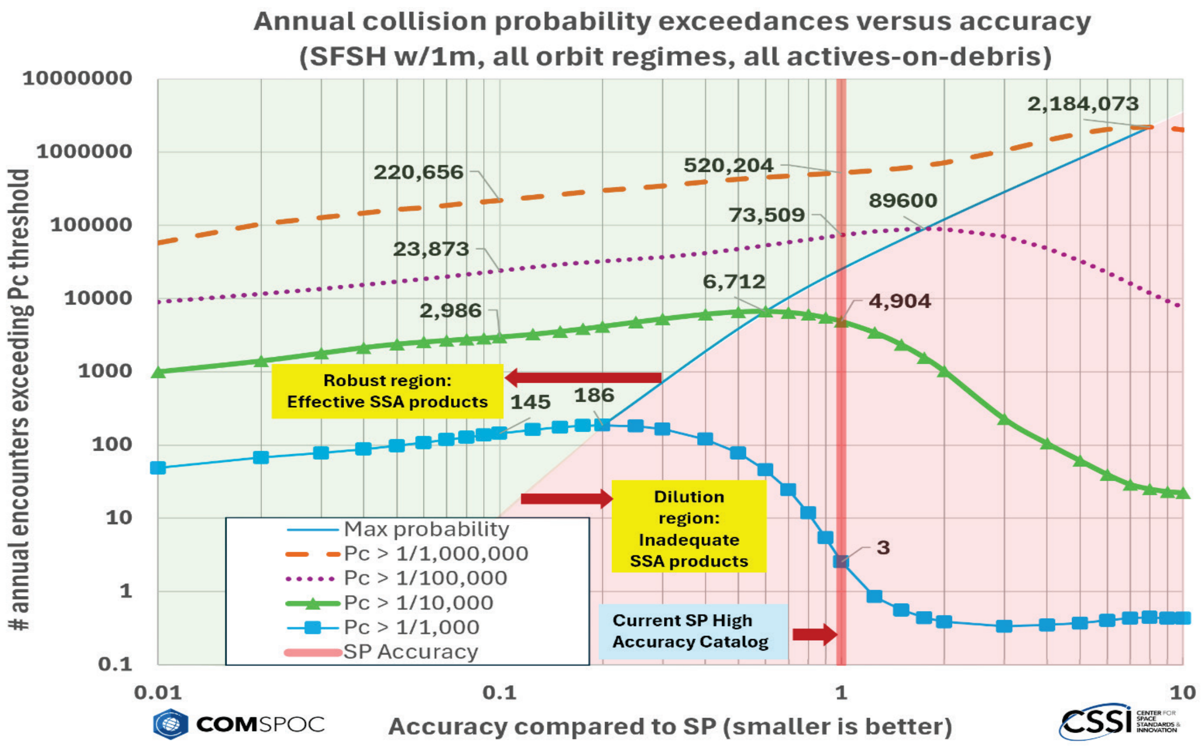

Figure 24: Annual Pc exceedance rate vs scale factor, depicting robust and dilution regions with numerical labels (SFSH HBRs gap-filled with 1m)

7. Estimating probability-based screening Type I and Type II errors

7.1. Assessment via the Mahalanobis probability threshold method

As is true with any method of determining action thresholds for operational use in identifying satellite conjunctions of significance, the quality of the data being used for such discriminations will have an outsized influence on the reliability of event detection. Reference [16] provides a qualitative study of this sensitivity for the Mahalanobis method outlined above, as well as other common methods.

When operationally implementing such a detection system, the decision makers must balance their choice of a detection threshold with the quality of available data to support it. Their ability to handle the operational tempo of mitigating realistic threats is impacted by the occurrence of misdiagnosed threats, which are typically categorized as Type I errors (“false alarms”) and Type II errors (“missed threats”).

If one adopts the Mahalanobis probability threshold method described in the previous section (or any detection method, for that matter), it is imperative to understand the impact of data quality on both reliability of mitigation (avoidance of Type II errors) and the unnecessary operational load imposed by Type I errors. This paper’s goal has been to numerically estimate the sensitivity of detection errors AND the effectiveness of avoiding collisions to data quality to allow operators to wisely choose their trigger limits. It is also illustrative to consider the circumstances of how these types of errors could occur while using the Mahalanobis probability detection threshold method with inputs of varying quality.

The Mahalanobis probability threshold method has three inputs that are subject to varying accuracies: the combined hard body radius (CHBR), the estimated miss distance (Miss dist.), and the uncertainty covariance (Covar), as depicted in **Figure**

25. The CHBR can often be a conservative overestimate derived from the maximum dimensions of both objects. The estimated miss distance is more likely to be smaller than the value at the detection threshold probability due to the definition of the Gaussian distribution. The covariance estimate is more likely to be too large unless efforts are made to improve its accuracy. With the variability of these three parameters in mind, their contributions to the number of Type I and Type II errors can be discussed.

Type I errors (false alarms) can arise in cases of both high and low accuracy combined covariances. In the case of low accuracy (overly large) covariance, small miss distances and an overestimation of combined hard body radius can still contribute to enough intersection area to reach the probability threshold. These detections may eventually be eliminated as data improves nearer to the time of close approach. In the case of high accuracy combined covariances, it is natural that miss distances are statistically more likely to be nearer the centre of the Gaussian distribution. These types of false alarms are expected and will reduce as accuracy (represented by the covariance error matrix) improves as the time of close approach nears.

Type II errors (missed threats) can also arise in cases of both high and low accuracy combined covariances. A low-accuracy, overly large covariance can cause a conjunction with an otherwise accurate miss distance and hard body radius to be missed since probability density will be diluted. Type II errors can also arise even in the case of a well-known (small) covariance, but at a lower rate. Uncommonly large miss distances can cause an event to be missed by sampling a lower density portion of the probability density function, but these larger miss distances are statistically less likely due to the nature of Gaussian distributions.

In summary, while Type I and Type II errors can occur for high and low accuracy covariances, the number of both errors tends to decrease as accuracy improves.

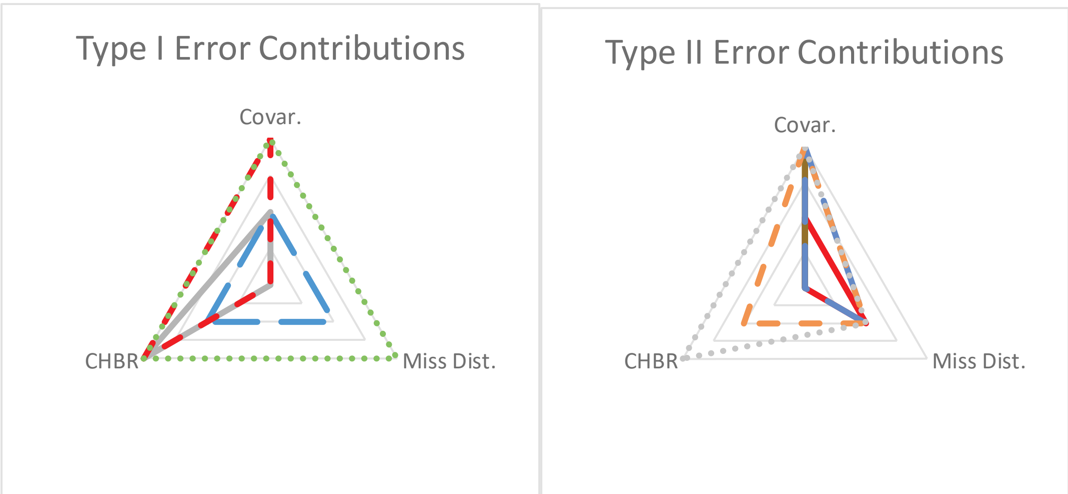

Figure 25: Notional chart illustrating the functional relationship between precision of the three parameters used in the Mahalanobis threshold filtering technique (covariance, miss distance, combined hard body radius) and potential Type I or Type II errors. Each triangle represents a combination of parameter accuracies, with the distance of a vertex from the center indicating the general size of that parameter (small to large). Color and line type are used to distinguish each triangle.

8. Evaluation of missed real collision risk

If one interprets the number of conjunction messages as a proxy for how much work the satellite operators and SSA systems need to perform, then **Figure 22**, **Figure 23**, and **Figure 24** are instructive:

a) Our current legacy SSA products and procedures are well into the dilution region, meaning that the data is not “fit for purpose” at one in ten thousand Pc screening threshold – in turn meaning that the estimated collision rates listed in Table 1 are not fully mitigated, and most of today’s collision avoidance processes may therefore be ineffective.
b) Were one to get better data, then more conjunctions would be flagged as being potential collision risks, thereby increasing satellite operator workload to remediate each one of them.
c) Were one to get still better data, the number of conjunctions having probabilities higher than the chosen probability threshold would drop.

But there is more to the story than simply trying to ease the spacecraft operator’s workload and that of the SSA system they use. Let’s now examine the impact of improving orbit positional knowledge on how much actual collision risk is retired.

For each RSO pair-wise collision risk identified by the Volumetric Encounter Rate tool, we can examine the probability one would estimate for that pair assuming a zero-miss distance coupled with the individual hard body radius (HBR) and synthetic covariance of each RSO.

Adoption of a zero-miss distance is justified because a non-zero collision rate requires the actual miss distance at the time of closest approach to be smaller than the combined HBR (CHBR), and CHBRs are typically on the order of a few meters. It turns out that a zero-miss distance assumption yields an optimistic estimate of how effective a probability-based screening against a threshold is, since incorporation of a non-zero miss distance for every collision risk would lower the collision probability estimate, leading to even more unretired collision risk.

We begin by identifying all conjunctions that come within the requisite distance which could potentially yield a collision probability that exceeds the collision probability threshold of interest: Assuming a combined covariance aspect ratio (AR) of 10 and a conservative combined hardbody radius of 30m, Pc thresholds of one in one million, one in one hundred thousand, one in ten thousand, and one in one thousand correspond to miss distance screening radii of 57km, 18km, 5.7km, and 1.8km respectively. These screenings were performed for all active-on-active, active-on-debris, and debris-on-debris pairings in the entire public catalog.

Our goal is to estimate the percentage of unretired collision risk, spanning all orbital regimes but only for RSO pairings that involve at least one active spacecraft, resulting from the selected collision probability threshold coupled with the quality of the SSA positional knowledge (represented by the same scale factor “S” applied to the synthetic covariances derived from SP ephemeris overlap statistics, where “S=1” denotes SP performance on 20 Feb 2026).

Our findings are shown in **Figure 26**. The estimated effectiveness of mitigating current collision risk using typical conjunction assessment SP products combined with typical Pc thresholds of one in ten thousand is indicated by the label ❶ marker. **For this typical combination of SSA accuracy and Pc threshold of one in ten**

thousand, note that the spacecraft operator is only avoiding an estimated 7% of the actual hardbody-on-hardbody (direct hit) collision risk.

Meanwhile, Starlink has already adopted a more stringent collision probability screening threshold [19] of three in ten million. So in this study, we chose to evaluate something near to that, at one in a million (three times less stringent than Starlink's). The anticipated effectiveness of that is indicated by label ❷, where the combination of SP-like accuracy combined with this much more stringent screening threshold retires 75% of the total estimated collision risk, a far better circumstance than for Pc threshold of one in ten thousand.

Unfortunately, **Figure 22** (and similar) showed us that there is a high penalty for eliminating almost all the collision risk by using a more stringent collision probability threshold: there will be more potential collision risks to mitigate. While helping to ensure the effectiveness of a flight safety system, SSA analyst and spacecraft operator staff resources and computational capabilities can experience "**crisis fatigue**" using an overly stringent Pc threshold.

But what if the accuracy of SSA positional knowledge could be improved by a factor of ten, for example? Operational pathfinders [20,21,22] conducted by the government and commercial SSA companies have consistently shown that this is not only possible, but achievable (**Figure 20** and **Figure 21**). This is attained by using innovative and technically mature orbit determination processes, improved space weather, better analytics, data fusion tools, and deep collaboration ("crowdsourcing") between SSA centres, operators, and governments.

This brings up an interesting point: Such a factor of ten improvement in SSA accuracy while screening to a lower collision probability of one in one thousand (denoted by ❸) would not only decrease the number of conjunction alerts thirty-fold, but it would also retire an additional 15% of the risk that current operators typically fail to address (unfortunately, still leaving 78% unmitigated).

Sticking with a one in ten thousand criteria with ten times more accurate SSA retires an estimated 75% of the collision risk (❹) while adopting a one in a million Pc threshold (❺) eliminates 92% of the risk! But again, using such a low Pc threshold has operational risks, in that it can introduce "Crisis Fatigue" in staff and require many computational resources and potentially manoeuvring fuel.

Figure 27 and **Figure 28** show the corresponding depictions for DISCOS and SFSH gap-filled with 1m HBRs, respectively. While the DISCOS 1m gap-fill did not appreciably alter the plot, the encapsulating sphere used in the SFSH dataset changed the trends greatly.

Note how in **Figure 28** the application of overly conservative HBR values greatly increases the collision avoidance effectiveness when using more accurate SSA data, even when using a relatively coarse Pc threshold of only one in one thousand! But there is a caveat on this result: When using median HBRs based upon the DISCOS data, it was reasonable to assume that the volumetric encounter rate mapped to CHBR distances well represents what the actual collision risk is. But in the case of the SFSH's "encapsulating sphere," that is not a good assumption to make because the actual hardbody cross-sectional area is likely to be 4X less (from ***Figure 3***). Accordingly, we tried to apply a 4X reduction factor to the collision rates to attempt to approximate the actual estimated collision risk, but this was unsuccessful. We recommend that this be a topic for further discussion and study.

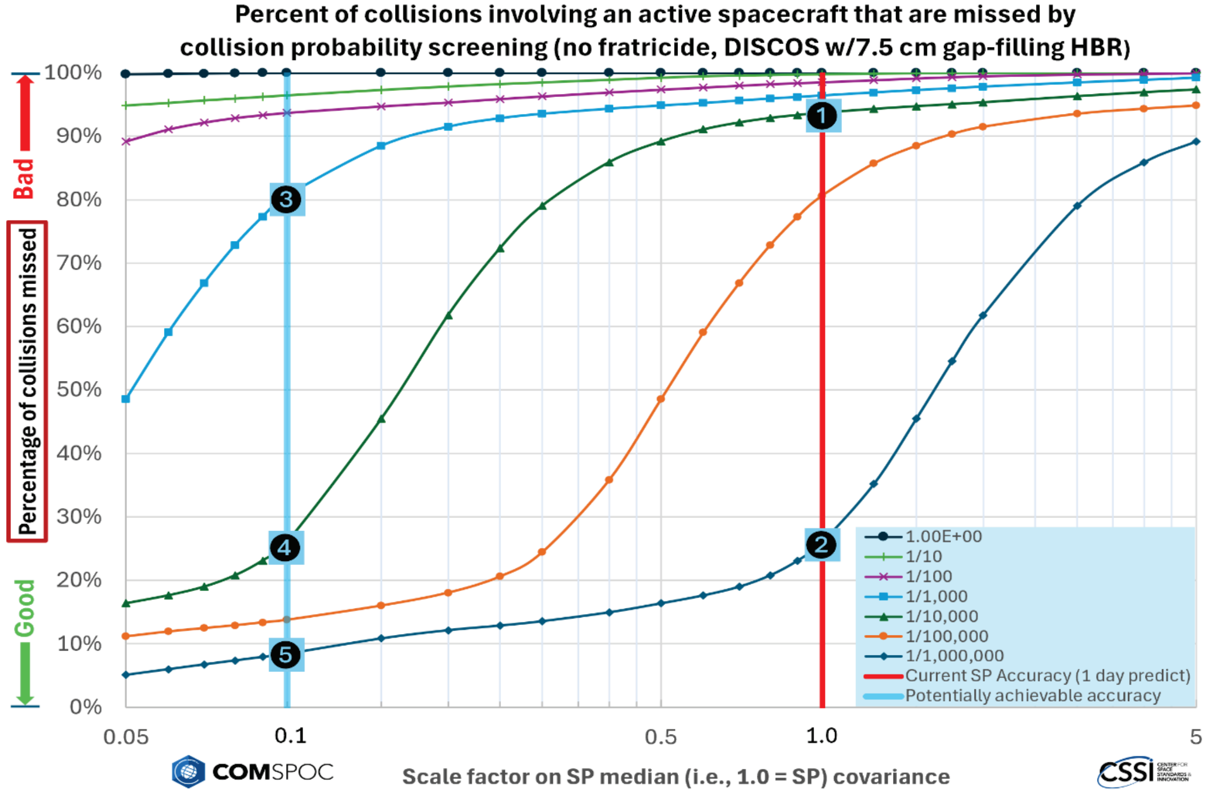

Figure 26: Percentage of UNRETIRED collision risk as a function of Pc threshold and SP covariance scale factor "S" (S<1 denotes improved accuracy over SP), using DISCOS HBRs gap-filled with 7.558 cm.

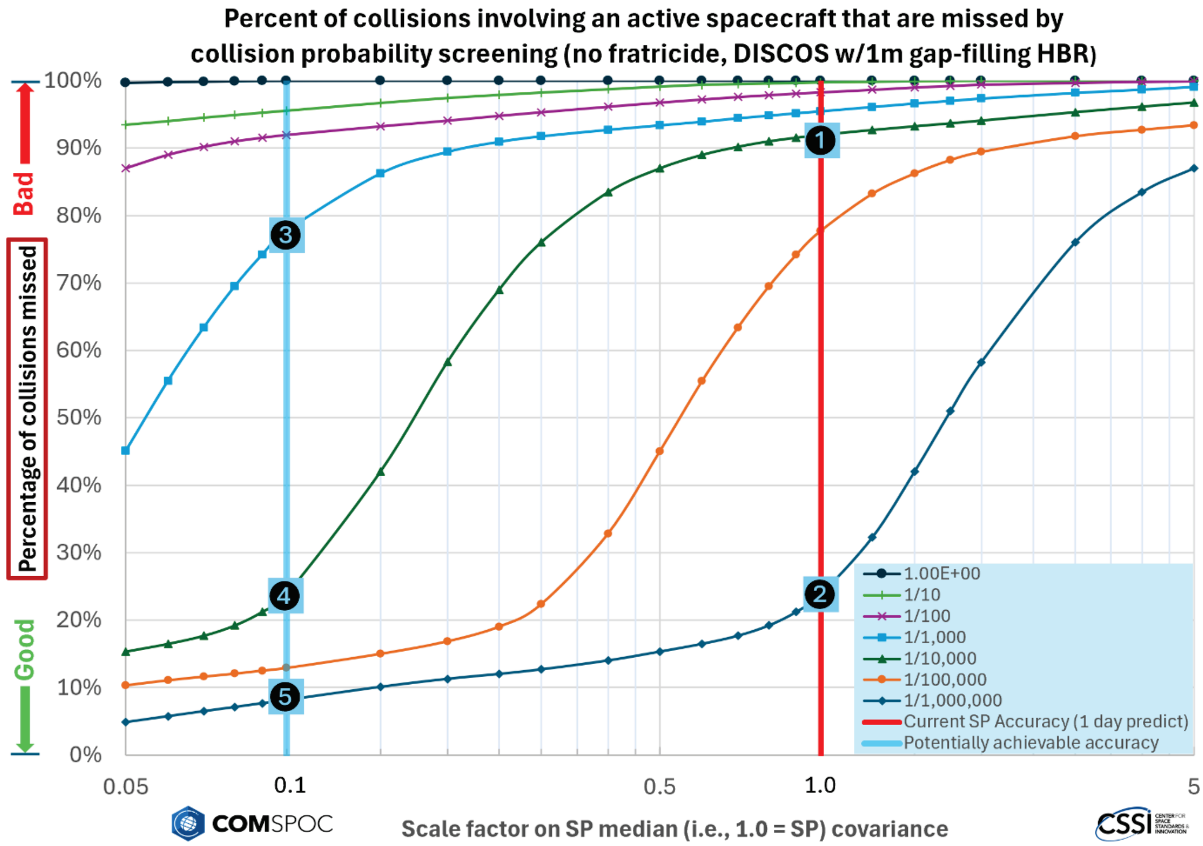

Figure 27: Percentage of UNRETIRED collision risk as a function of Pc threshold and SP covariance scale factor "S", using DISCOS HBRs gap-filled with 1m.

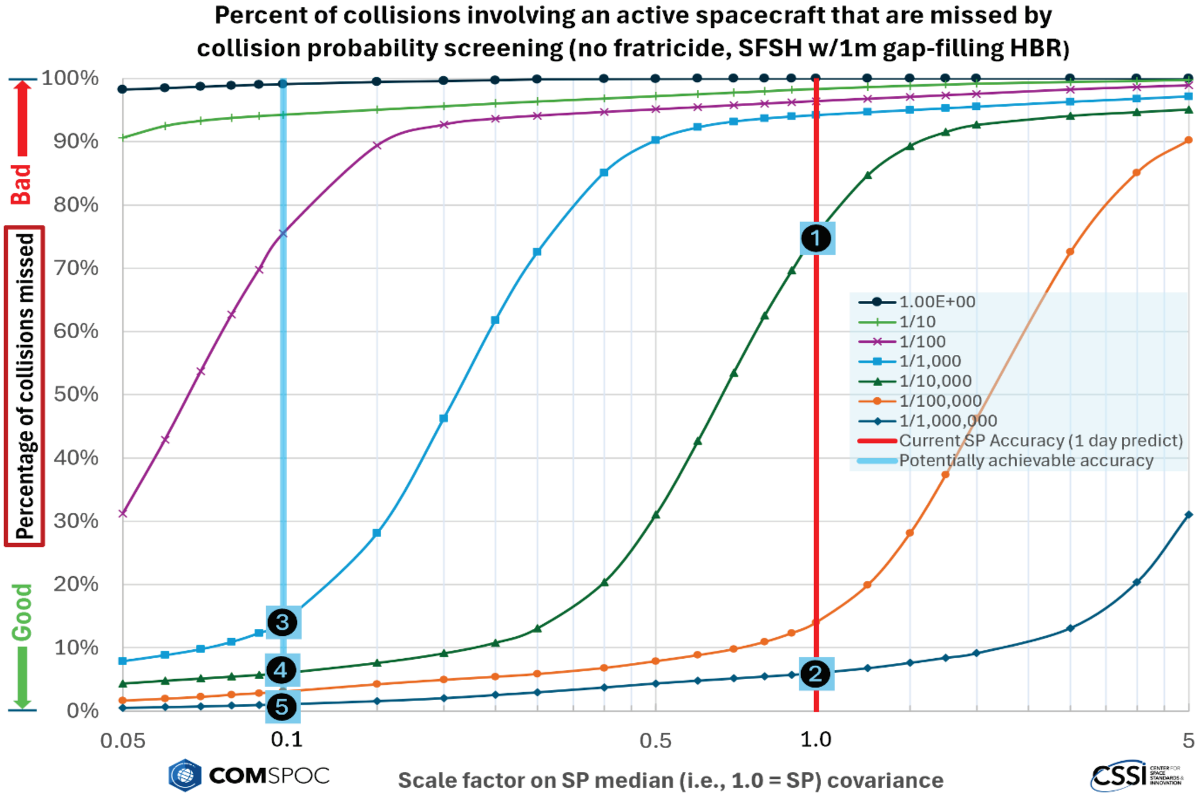

Figure 28: Percentage of UNRETIRED collision risk as a function of Pc threshold and SP covariance scale factor "S", using SFSH HBRs gap-filled with 1m, "normalized to an encapsulating sphere encounter rate."

9. CONCLUSIONS

The combination of the estimated Pc encounter rates and retired risk percentages as a function of the SSA positional knowledge "S" factor indicate that typical operators today are only retiring 7% of the collision risk due to their selected collision probability threshold coupled with legacy SSA accuracy.

Employing a more stringent collision probability threshold and then improving accuracy by a factor of ten can reduce the number of warnings by more than 50% while retiring at least 75% of the total risk. Therefore, adoption of a more stringent Pc threshold coupled with a tenfold improvement in SSA accuracy is seen as being essential to achieving a truly effective space safety process.

If we fail to prevent them effectively, collisions between satellites within a constellation (fratricide), represents greatest collision risk. In today's world, we are increasingly at a crossroads between space flight safety and today's hostile actions: an attacker's cyber-attack in time of conflict could render a large constellation of spacecraft unmanageable. Threats to large constellations (also including a Carrington-type event, nuclear weapon detonation in space, directed energy technologies [23,24,25] or other such weapons should be taken very seriously and avoided.

We also found that if collision avoidance procedures and SSA data render collision avoidance ineffective, our collision rate characterization indicates collisions every five years between debris objects, and in the absence of fratricide, collisions between spacecraft operated by two different operators represents 61% of the total estimated collision risk with two hardbody collisions per year involving active spacecraft, and one collision annually between an active spacecraft and debris.

Approximately 6% of the aggregate total collision risk occurs between two debris objects and can only be addressed by an active debris removal capability. Note that while we focused on only collision rates, the risk (a product of probability and consequence) of collision between two debris objects depends upon the mass of each object and anticipated fragmentation effects on space sustainability.

The findings also emphasize the critical need to realize a comprehensive and complete globally accessible spacecraft size and dimensions database.

10. FUTURE WORK

We plan to explore the fundamental relationships and assumptions adopted herein. We will also determine if using many lower-quality observations (e.g., star-tracker based, solving orbits using a variety of OD methods and the accompanying en masse calibration efforts that such voluminous set of sensors would require) works better than using fewer exquisite sensors having less observations (but higher accuracy). We will examine how encapsulating sphere HBRs can better be accommodated in this assessment. Additionally, incorporating space object mass and degradations to the space environment would also be of key interest. Furthermore, we suspect that many of the Range Operating Characteristic (ROC) curve relationships identified in [14] and seen in this paper might also be present in military applications for SSA data (not only space flight safety); therefore, we would like to investigate whether a similar approach could address challenging military problems.

11. ACKNOWLEDGEMENT

Our thanks to the European Space Agency for allowing access to their DISCOS database, which provides global insights into the shape, size, and mass of active and inactive spacecraft and debris. Our thanks also to the Spacebook.com team for providing access to Two-Line Elements (TLEs) which were used to estimate long-term collision rates. And finally, our thanks to United States Space Force, for their continued sharing of their Special Perturbations (SP, also known as High Accuracy Catalog, or HAC) ephemerides, from which we were able to estimate median SP covariances one day after Orbit Determination (OD) epoch.

Also, note that this research draws upon information from the ESA DISCOS (Database and Information System Characterising Objects in Space), a single-source reference for launch information, object registration details, launch vehicle descriptions, as well as spacecraft information for all trackable, unclassified objects. We acknowledge ESA's efforts to maintain and operate this database with its APIs.

12. REFERENCES

[1] Sánchez-Ortiz, N., Domínguez-González, R., and Krag, H., “Evaluation of minimum coverage size and orbital accuracy at different orbital regimes for one order of magnitude reduction of the catastrophic collision risk,” 15 Mar 2015, accessible at https://doi.org/10.1016/j.asr.2014.12.034

[2] R.G. Gist, D.L. Oltrogge, S. Alfano, “Synthetic Covariance Production Using a New Digital Approach,” IAA-ICSSA-24-0000, IAA STM Conference on SSA, 8 May 2024, Embry-Riddle University, Daytona Beach, Florida.

[3] Oltrogge, D.L., Getz, G., Vallado, D.A., Alfano, S., Gist, R.G., Shogren, S., "Using Spacebook and Cesium to Promote and Enhance Flight Safety," European Conference on Space Debris, Bonn, Germany, 2 April 2025.

[4] Alfano, S., Oltrogge, D.L., Krag, H., Merz, K., and Hall, R.H., “Risk assessment of recent high-interest conjunctions,” Acta Astronautica 2021, https://doi.org/10.1016/j.actaastro.2021.04.009, 7 April 2021.

[5] DISCOS (Database and Information System Characterising Objects in Space) https://discosweb.esoc.esa.int.

[6] Email from U.S. Department of Commerce’s Office of Space Commerce, “OSC Publishes Conjunction Assessment Dataset,” dated 24 March 2026, with the database accessible on a full and open basis, with no restrictions on use or dissemination, under the Creative Commons Universal Public Domain Dedication (CC0-1.0), at: https://space.commerce.gov/dataset-for-conjunction-assessment-verification/.

[7] S. Alfano and D.L. Oltrogge, "Volumetric assessment of satellite encounter rates,” Acta Astronautica, Volume 152, 2018, pp. 891-907, DOI: 10.1016/j.actaastro.2018.09.030

[8] Oltrogge, D.L., Alfano, S., Wilson, J. and Wauthier, P., “Evaluation of LEO conjunction rates using historical flight safety systems and analytical algorithms,” IAC-21-A6.7x65213, 72nd International Astronautical Congress (IAC), Dubai, United Arab Emirates, 25-29 October 2021.

[9] D.L. Oltrogge, S. Alfano, C. Law, A. Cacioni, and T.S. Kelso, “A comprehensive assessment of collision likelihood in Geosynchronous Earth Orbit," Acta Astronautica (2018), doi:10.1016/j.actaastro.2018.03.017.

[10] Oltrogge, D.L., Alfano, S., Vallado, D.A., Zimmer, P., Hall, R.H., Wilson, J., Siegers, M., and Aurich, J., “Russian ASAT Debris Cloud Evolution and Risk,” 3rd IAA Conference on Space Situational Awareness, Madrid Spain, 4-6 Apr 2022.

[11] S. Alfano, D.L. Oltrogge, and L. Arona, “SSA positional and dimensional accuracy requirements for Space Traffic Coordination and Management,” AMOS Conference, Maui, Hawaii, 14-17 September 2021.

[12] SPACEBOOK website, https://spacebook.com/.

[13] Oltrogge, D.L. and Alfano, S., “Collision Risk in Low Earth Orbit,” IAC-16, A6,2,1,x32763, 67th International Astronautical Congress, Guadalajara, Mexico, 26-30 September 2016.

[14] Alfano, S. and Finkleman, D., “Operating characteristic approach to effective satellite conjunction filtering,” AAS 13-435, 2013.

[15] P.C. Mahalanobis, “On the generalised distance in statistics,” Proceedings National Institute of Science, India, Vol. 2, No. 1. (16 April 1936), pp. 49-55.

[16] S. Alfano and D.L. Oltrogge, "Probability of Collision: Valuation, Variability, Visualization, and Validity,” Acta Astronautica, Volume 148, July 2018, pp. 301-316, DOI: 10.1016/j.actaastro.2018.04.023

[17] F. K. Chan, Spacecraft Collision Probability, The Aerospace Press, El Segundo, 2008.

[18] S. Alfano, "Relating Position Uncertainty to Maximum Conjunction Probability”, AAS Journal of the Astronautical Sciences, Vol. 53, No. 2, April-June 2005, pp. 193-205.

[19] Goldman, D., “SpaceX Gen 1 and Gen 2 Semi-Annual Reports,” SpaceX report to M. Dortch of the FCC, dated 31 December 2025.

[20] Oltrogge, D.L., Wauthier, P., Vallado, D.V., Alfano, S., and Kelso, T.S., “Results Of Comprehensive STCM Data Fusion Experiment,” Proc. 8th European Conference on Space Debris (virtual), Darmstadt, Germany, 20-23 April 2021, https://conference.sdo.esoc.esa.int/proceedings/sdc8/paper/263/SDC8-paper263.pdf (accessed 30 September 2021).

[21] Oltrogge, D.L., Chan, J., Vallado, D.A., Cornelius, J., D'Uva, A.R., Hall, R.A., “Deep Operator and SSA Collaboration for Space Sustainability”, 12th IAASS Conference, Osaka, Japan, 23 May 2023.

[22] Oltrogge, D.L., Chan, J., Vallado, D.A., Cornelius, J.J., D’Uva, A., and Hall, R.A., “Deep operator and SSA collaboration for space sustainability,” Journal of Space Safety Engineering Vol II, Issue 2, June 2024, pp. 342-361, freely downloadable at: https://doi.org/10.1016/j.jsse.2024.03.007.

[23] Secure World Foundation, “Global Counterspace Capabilities: An Open Source Assessment,” accessed 17 March 2026 at: https://drive.google.com/file/d/1FxYfoY9eqUew3xL2LD__xgHVIOFVvASA/view?pli=1

[24] SpaceNews, “Russia, China target SpaceX’s Starlink in escalating space electronic warfare,” Sandra Erwin, 3 April 2025, accessed 17 March 2026 at: https://spacenews.com/russia-china-target-spacexs-starlink-in-escalating-space-electronic-warfare/

[25] “Starlink killer: China’s new microwave weapon,” Firstpost, accessed 17 March 2026 at: https://www.youtube.com/watch?v=P6G4bDbdURU

